A Wien Filter velocity analyzer for intermediate energy electron impact spectroscopy

Heloisa M. Boechat-Roberty* and Gerardo Gerson B. de Souza

Instituto de Química, Universidade Federal do Rio de Janeiro

Cidade Universitária, 21910, Rio de Janeiro Brazil

* *Observatório do Valongo, Universidade Federal do Rio de Janeiro*

Ladeira Pedro Antônio 43, 20080 - 090, Rio de Janeiro, Brazil

Recebido em 13 de junho, 1995

A new electron velocity analyzer based on the Wien Filter principle, has been developed. In this analyzer an electrical and magnetic field perpendicular to each other, disperse electrons of different energies. Immersion electrostatic lenses are employed, in order to decelerate and accelerate the electrons respectively before and after energy dispersion. This analyzer has demonstrated an excellent capability in the determination of energy-loss spectra in an extended impact energy range (0.2 to 1.5 keV). The high inherent signal/noise ratio has lead to the acquisition of well-defined and reliable inner-shell excitation spectra

Foi desenvolvido um novo analisador de velocidades de elétrons baseado nos princípios do Filtro de Wien. Este analisador utiliza campos elétrico e magnético perpendiculares para separar elétrons de energias diferentes. Foram empregadas lentes eletrostáticas de imersão para desacelerar e acelerar elétrons antes e depois da região de dispersão, respectivamente. Este analisador demonstrou uma excelente capacidade para a determinação de espectros de perda de energia em um extenso intervalo de energia de impacto (0.2 a 1.5 keV). A alta relação sinal/ruído tem permitido a obtenção de espectros de excitação de camada interna.

1. Introduction

The use of electrical and magnetic field perpendicular to each other, to select velocities of charged particles began with Wien[1] in 1902. Herzog[2] (1934), using the fundamental equations to describe the charged particles trajectories under the action of electric and magnetic forces, demonstrated that this field combination results in an electro-optical device with the same properties of an optic lens. The Wien Filter has also been employed with success as a mass separator, for example, in isotope separation in nuclear reactions[3] and in the study of spatial plasmas[4,5], on board of a spacecraft. As an electron velocity analyzer, the Wien Filter has been employed in electron microscopy[6,7] in coincidence experiments (e,2e)[8] and in the investigation of the electronic structure of solids[9]. Leal-Quiros et al.[10] designed two Wien filters to work as electron energy analyzer and as mass analyzer. They concluded that it has a much higher mass and energy resolution than do conventional mass and energy analyzers. In the area of electron energy-loss spectroscopy (EELS) the pioneer work of Boersch et al[11,12] must be emphasized. Using a Wien filter both as analyzer and as monochromator, they achieved a very high energy resolution (17 meV at an impact energy of 25 keV).

In the present paper we describe a Wien Filter velocity analyzer designed and constructed to select scattered electrons in gas phase experiments performed in the impact energy range from 0.1 to 3.0 keV. The choice of this analyzer type was motivated by the very high energy resolution which has been reported by Boersch et al[11] as well as by its straight optic axis what allows a much simpler system alignment as compared with systems with curved axis geometries such as hemispherical and 127° velocity analyzers.

2. Theory

The Wien Filter uses an electrostatic field **E** perpendicular to a magnetic field **B** to disperse electrons of different energies, based on the following principle. Electrons with velocity $v_0 = |\mathbf{E}|/|\mathbf{B}|$ pass perpendicularly through the crossed fields without to change in its trajectories (along the optical axis), because the electric and magnetic forces are mutually canceled. Electrons with different velocities

$$v = v_0(1+\beta) \tag{1}$$

will be deflected from the optic axis[13], where β is the velocity deviation. The trajectory radius of the electrons with velocity v_0 upon action of the magnetic field would be given by

$$\rho = \frac{m|v_0|}{e\mathbf{B}} \tag{2}$$

where m and e are the mass and charge of the electron respectively. The electric force modifies this trajectory. The electron equation of motion under action of the electric and magnetic fields is given by

$$m\ddot{r} + e\mathbf{E} + e(v \times \mathbf{B}) = 0 \tag{3}$$

Let us assume rectangular coordinates, where the x-axis is in the direction of the incoming electron, the y-axis and z-axis are in the directions of the the electrostatic field and the magnetic field respectively. The dispersion plane is the xy plane. The solutions equation (3) are obtained considering the initial conditions, i.e. how the electrons enter in the crossed fields region. First of all, we consider that at t=0, the entrance position with respect to the optic axis is y_0 and the entrance angle is α (both are experimentally defined by the entrance slits). The electron velocity is given by (1). Secondly, we assume that the fields are present only in the analysis region and consequently edge effects are neglected. In addition, the α angle is assumed to be too small so that we need to take into account only the first order term. The we have the following solutions[13]

$$x = -y_0 \sin\left(\frac{v_0 t}{\rho}\right) + \rho\alpha \cos\left(\frac{v_0 t}{\rho}\right) + \rho\beta \sin\left(\frac{v_0 t}{\rho}\right) + v_0 t - \rho\alpha$$

$$y = y_0 \cos\left(\frac{v_0 t}{\rho}\right) - \rho\beta\left\{1 - \cos\left(\frac{v_0 t}{\rho}\right)\right\} + \rho\alpha\left(\frac{v_0 t}{\rho}\right)$$

When the approximations $\alpha \ll 1$, $\beta \ll 1$ and $y_0 \ll L$ (L is the length of the crossed fields region) are made, we have

$$x = v_0 t = L \tag{4}$$

and we can then write

$$y = y_0 \cos\left(\frac{L}{\rho}\right) + \rho\alpha \sin\left(\frac{L}{\rho}\right) + \rho\beta\left\{\left(1 - \cos\frac{L}{\rho}\right)\right\} \tag{5}$$

where y refers to the displacement from the optic axis. The first term in equation (5) shows the dependence on the entrance slits dimension, i e., the source size y_0, the second gives information about the angular blurring caused by the α angle and the third term, the most important, represents the dispersion of the electrons as a function of their velocity. From equation (5) we get that the highest dispersion will occur when

$$\frac{L}{\rho} = n\pi \tag{6}$$

for $n = 1, 3, 5$, etc. Using condition (6) in (5) for $n = 1$, (since at this condition we have the highest dispersion)[13], putting β in term of the energy, ($\beta = 1/2(\Delta\epsilon/\epsilon_0)$ and assuming that $y_0 \ll L$ the dispersion relation can then be obtained

$$y = \left[\frac{L}{\pi}\right]\frac{\Delta\epsilon}{\epsilon_0} \tag{7}$$

where $\Delta\epsilon$ is the absolute energy resolution and ϵ_0 is the pass energy. Expression (7) shows that to a lower pass energy corresponds a higher dispersion and that electrons with different energies will leave the filter at different positions due to chromatic aberration.

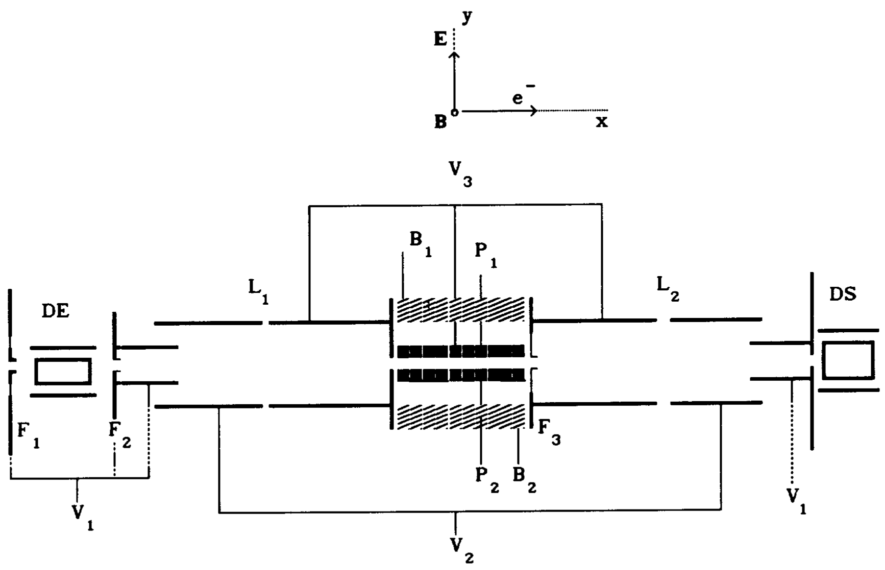

Figure 1 - Wien Filter analyzer scheme

L_1 - Deceleration Lens
L_2 - Acceleration Lens
F_1 - First Entrance Slit
DE - Entrance Deflectors
F_2 - Second Entrance Slit (current measurement)
V_1 - Low Voltage Elements of the lenses
V_2 - Focusing Lenses Elements
V_3 - High Voltage Elements of the lenses
F_3 - Exit Slit
DS - Exit Deflectors
P_1,P_2 - Parallel Plates (Electric Field)
B_1,B_2 - Coil End (Magnetic Field)
Coil Representation
e^- Electrons beam

3. Design

The basic parameters used in the design of the present analyzer are outlined in Table 1.

The crossed fields region is placed between two immersion electrostatic lenses, L_1 and L_2, for deceleration and acceleration of the electrons before and after the analysis region (Fig. 1). This arrangement allows the velocity analysis to be done at low kinetic energies, consequently increasing the dispersion power. Reacceleration is required in order to increase the detection efficiency.

3.1. Crossed field region

The electrostatic field is generated by two parallel brass plates P_1 and P_2 (Fig. 1) with length and width of 2.0 cm and 0.8 cm respectively, separated from each other by 0.4 cm. The length of the filter is L = 20 cm. An electric field of 63.7 V/cm is obtained for a potential difference of 26 V between the plates. The plates were polished and gold plated to guarantee the electric field uniformity and to avoid oxidation in contact with air or corrosives gases.

The magnetic field is produced by a toroidal winding with a gap of 1.0 cm. The coil nucleus was constructed from aluminum to allow a zero magnetic field when the electric current is null. A field of approximately 24 gauss acts across the gap when an electric current of 240 mA is fed. The deflectors plates, electrically isolated, were set up at the toroidal gap and between the high voltage lens elements V_3.

Table 1 - Wien Filter analyser: basic parameters

Pass Energy	$\epsilon_0 = 20$ eV
Length of the Filter	L = 2. 0 cm
Magnectic Field	B = 24 gauss
Electric Field	E = 63.69 V/cm
Electron velocity	$\|v_0\| = 2.65 \times 10^8$cm/s
Distance between the plates	d = 0.4 cm
Electron orbit radius	$\rho = 0.64$ cm
Energy Dispersion	318 μm/eV

3.2. Electrostatic lenses

The two cylindrical electrostatic lenses L_1 e L_2 were designed and the electron optic principles (Spangemberg[14] and Harting and Read[15]). Two asymmetric three elements electrostatic lenses, V_1, V_2, V_3, i. e., zoom lenses, are employed. In this type of lens the ratio V_3/V_1 is responsible for the electron energy change and the ratio V_2/V_1 is responsible for the focusing. The simultaneous scanning of V_2 and V_3 allows the deceleration and acceleration of the electrons while maintaining a fixed focal point position. The deceleration lens L_1 and acceleration lens L_2 are similar to each other, and both have been made out of brass. At the first lens L_1, the element V_1 is a cylinder of 1.2 cm of diameter and 1.0 cm length. Both the elements V_2 and V_3 have diameter $D = 1.6$ cm and lengths of 1.6 and 3.0 cm respectively, separated by $g = 0.16$ cm, i. e., 10% of the diameter D. The elements of the acceleration lens L_2 have the same dimensions of L_1 but are placed in an inverted sequential position, i.e., V_3, V_2 and V_1. The surfaces of the lenses that are exposed to electrons are coated with colloidal graphite.

The electrons trajectories at the electrostatic lenses have been simulated using the SIMION computer program, (Idaho National Engineering Laboratory). The simulations have shown that the expected zoom behavior has been attained. For example, figure 2 shows that electrons which have been decelerated from (a) 980 eV and (b) 930 eV to 25 eV are focused at the same position.

The acceptance angle α for the electrons at the entrance of lens L_1 is defined by the two circular slits F_1 and F_2 separated by 2.0 cm. In the present measurements the two slits are 500 μm in diameter. Two pairs of deflectors plates (DE), were put between the first and second slits in order to correct the position axis of the system. The electrically isolated aperture F_2 can be used to measure the beam current; minimization of the current corresponds to the maximization of the number of electrons passing through the slits. An energy selecting slit F_3 is placed at the exit of the analysis region. After the last element of the acceleration lens L_2 two additional pairs of deflectors (DS) have been placed to position the electrons on the detector slit.

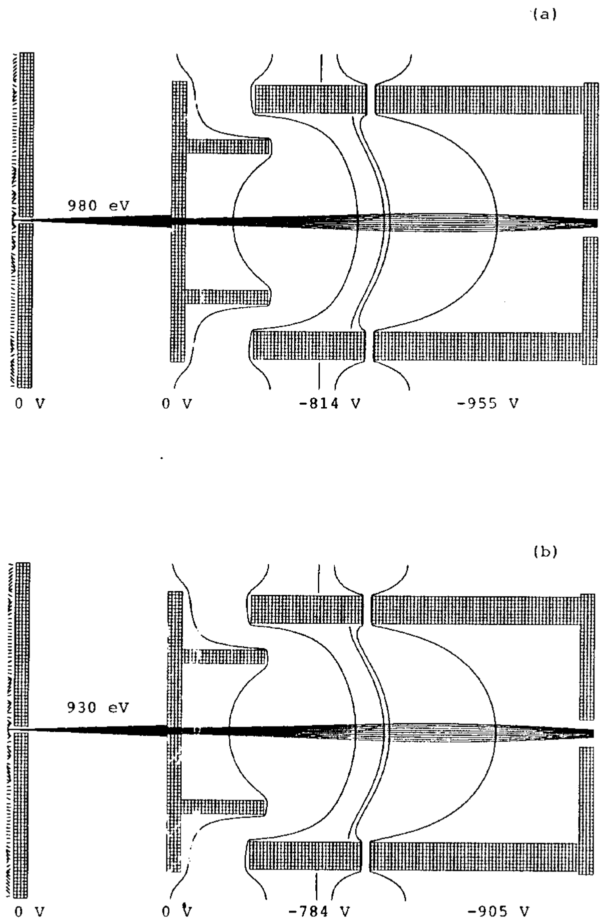

Figure 2. Electrostatic lens. Electrons which have been decelerated from (a) 980 eV and (b) 930 eV to 25 eV are focused at the same position.

4. Performance

In the present instrument, constant pass-energy-mode is used, i.e., the analyzer is set to transmit only electrons which have a specific energy $\epsilon_0 = 1/2\ m\ v_0^2$, defined by the electric $\mathbf{E}$ and magnetic fields $\mathbf{B}$ applied. Scanning the lens voltages (V_2, V_3) provides focusing and deceleration of the electrons of different energies ϵ to a fixed pass-energy ϵ_0. Electrons with different energies are dispersed from the optic-axis and are cut out by the energy selecting slit F_3. The selected electrons are re-accelerated to their incoming energy. As shown in figure 1, each pair of similar elements of the two lenses have been electrically connected, allowing a simultaneous voltage scanning.

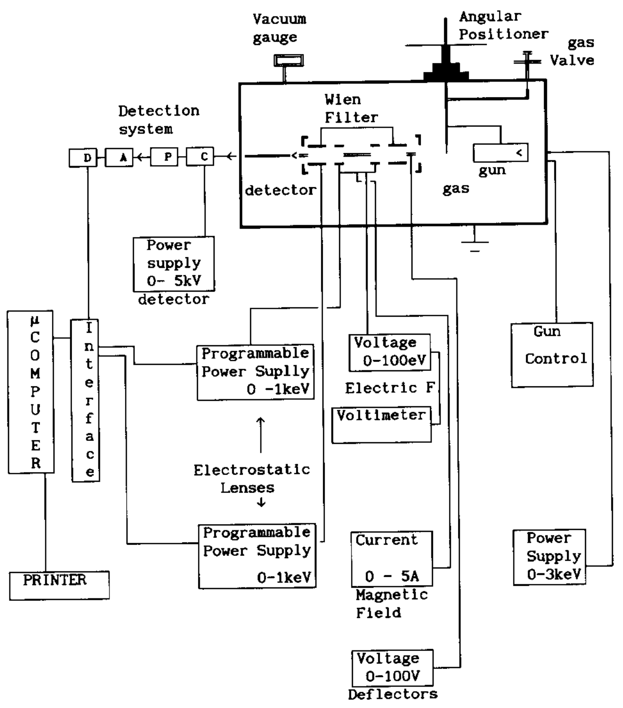

Figure 3. Electron Impact Spectrometer with Wien Filter Analyzer. (Ref. 17).

The Wien filter analyzer was incorporated into an energy-loss spectrometer that has been described before[16], and the complete system is shown schematically in Fig. 3 (Ref. 17). This apparatus employs a crossed-beam technique, where the thermionically produced electron beam, (with an energy range of 0.1 to 3.0 keV) is focused to a 1mm spot by means of an electrostatic lens and collides with an atomic or molecular gaseous beam. The scattered electrons are analyzed by the Wien Filter analyzer and subsequently are detected by an electron multiplier (Spiralton, Galileo Electro Optics). The pulses coming out of the detector are fed to a standard electronics (preamplifier, amplifier, discriminator) and are then transferred to the memory of the 16-bit personal microcomputer which is also responsible for the scanning of the voltages applied to the zoom lenses.

In our apparatus a high negative voltage is applied to the electron gun filament and the spectrometer is held at ground potential, therefore V_1 is also maintained at ground potential.

The Wien Filter analyzer has demonstrated excellent capability in the determination of the energy-loss spectra in an extended impact energy range (0.2 to 1.5 eV). Figure 4 shows the energy-loss spectra for the Argon atom, obtained at an impact energy of 1.0 KeV and 210 eV. For a given slit size the resolution is dependent on the pass energy. We obtained, for example an energy resolution of 0.7 ± 0.1 eV for a pass energy of 22.0 eV in the impact energy of 1.0 KeV, as determinated by the full-width at half maximum for the zero-energy-loss elastic peak.

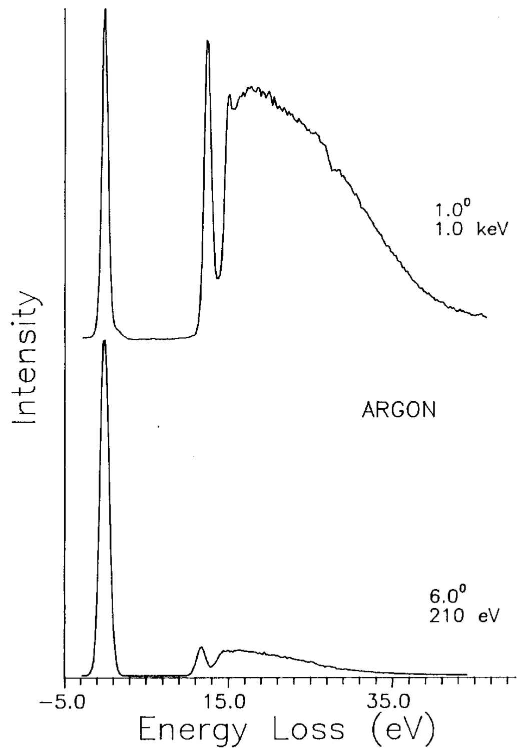

Figure 4. The energy-loss spectra for the Argon atom. The energy resolution are 0.7 eV for 1.0 keV and 1.4 eV for 210 eV.

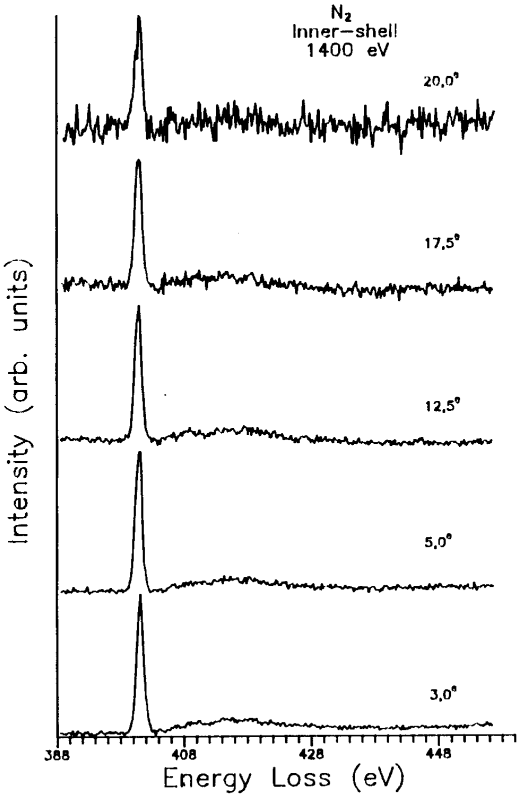

Figure 5. The inner-shell energy-loss spectra of the N_2 molecule.

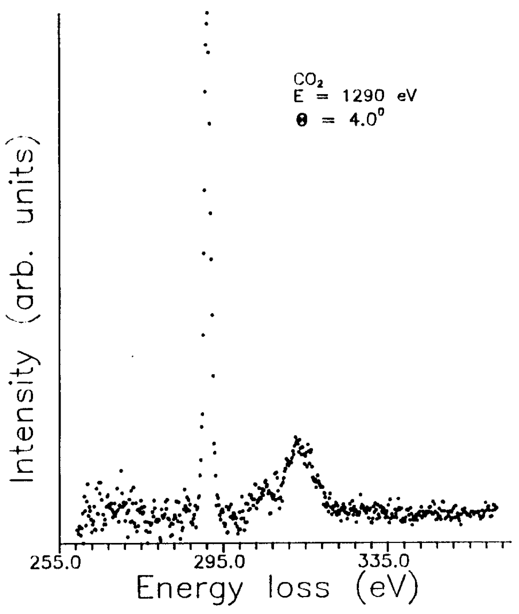

Figure 6. Energy-loss spectrum of $C0_2$. The intense peak refers to the (Cls)$2\sigma_g \rightarrow 2\pi_u$ transition. (Ref. 17)

The analyzer has also been successfully employed on the measurement of angle-resolved electron energy-loss spectra for inner-shell excitation in several molecules such as N_2 CO_2 (Ref. 17), C_2H_2 (Ref. 18). Figure 5 shows that the N1s excitation spectrum in the N_2 molecule is dominated by the $N1s \rightarrow \pi^*$ transition in the 3° to 20° angular range. The C1s ($2\sigma_g \rightarrow 2\pi_u$) transition in the $C0_2$ molecule is shown in figure 6. The generalized oscillator strength (GOS) for the latter transition, as well as for the C1s ($1\sigma_g \rightarrow 1\pi_g$) and C1s ($1\sigma_u \rightarrow 1\pi_g$) transitions in the C_2H_2 molecule have been determined as a function of the square of the momentum transfer, K^2 and these results have been presented elsewhere (Boechat-Roberty et al[17] and Miranda et al.[18] respectively).

5. Conclusions

The Wien Filter electron velocity analyzer has been built and demonstrated an excellent capability in the determination of electron energy-loss spectra in an extended impact energy and scattering angle range. A high signal/noise ratio has made possible the measurement of angle-resolved electron energy-loss spectra and generalized oscillator strength for inner-shell excitation in atoms and molecules.

Acknowledgements

We would like to acknowledge the financial support of the Conselho Nacional de Desenvolvimento Científico e Tecnológico (CNPq) and the Financiadora de Estudos e Projetos (FINEP). The authors also thank C. A. Lucas for his help during the testing of the analyzer.

References

1. W. Wien, Ann. Physik **8**, 260 (1902).
2. R. Herzog, Z. Physik **89**, 447 (1934).
3. L. Wahlin, Nucl. Inst. and Meth. **27**, 55 (1964).
4. K. W. Olgivie, N. Macllwraith, T. D. Wilkerson, Rev. Sci. Instr. **39**, 441 (1968).
5. K. W. Olgivie, R. I. Kittredge, Rev. Sci. Inst. **39**, 459 (1968).
6. P. E. Batson, Scan. Elect. Microsc. **I**, 15, 7 (1985).
7. P. E. Batson, Rev. Sci. Instr. **57**, 43 (1986).
8. A. L. Ritter, J. R. Dennison, J. Dunn, Rev. Sci. Instr. **55**, 1280 (1984).
9. H. Zscheile, J. Phys. E: Sci Instr. **15**, 749 (1982).
10. E. Leal-Quiros and M. A. Prelas, Rev. Sci. Instrum. **60**, 350 (1989).

11. H. Boersch, J. Geiger, H. Hellwig, Phys. Letters **3**, 64 (1962).
12. H. Boersch, J. Geiger, M. Stickel, Z. fur Phys. **180**, 415 (1964).
13. R. A. Bonham, M. Fink, *High Energy Electron Scattering*, Van Nostrand-Reinhold, (1974).
14. K. R. Spangernberg *Vacuum Tubes*, McGraw-Hill (1948).
15. E. Harting, F. H. Read *Electrostatic Lenses*, Elsevier Scientific Publishing Company (1976).
16. G. G. de Souza, A. C. A. Souza, J. Phys. E **18**, 1037 (1985).
17. H. M. Boechat Roberty, C. E. Bielschowsky, G. G. de Souza, Phys. Rev. A **44**, 1694 (1991).
18. M. P. de Miranda, C. E. Bielschowsky, H. M. Boechat Roberty, G. G. de Souza, Phys. Rev. A **49**, 2399 (1994).